

Kinetic Investigations To Enable Development of a Robust Radical Benzylic Bromination for Commercial Manufacturing of AMG 423 Dihydrochloride Hydrate

James I. Murray,* Maria V. Silva Elipe, Andrew Cosbie, Kyle Baucom, Kyle Quasdorf, and Seb Caille



Cite This: *Org. Process Res. Dev.* 2020, 24, 1523–1530



Read Online

ACCESS |

Metrics & More

Article Recommendations

Supporting Information

ABSTRACT: During development of a radical benzylic bromination, observation of polymerized byproducts and variation in isolated yields warranted an in-depth mechanistic investigation to ensure process understanding and robustness. In situ kinetic studies using multinuclear CryoFree NMR spectroscopy revealed molecular bromine to be the active brominating species and variable time normalization analysis allowed accurate determination of the order of each reagent in this process. These kinetic studies allowed for accurate reaction modeling and were used to demonstrate that adoption of a simple procedural change ensured reliability and reproducibility during manufacturing.

KEYWORDS: benzylic bromination, radical chemistry, reaction kinetics, kinetic modeling

Radical benzylic brominations using *N*-bromosuccinimide (NBS) and a radical initiator have been utilized widely in the scientific literature since the first demonstration of this reaction by Alfred Wohl at the beginning of the 20th century.^{1,2} However, despite widespread use of this chemical transformation, there is still debate in the literature over the reaction mechanism, specifically, the identity of the active brominating species. In 1944, Bloomfield proposed that NBS was the active brominating agent and that the succinimidyl radical acted as the radical chain carrier (*Scheme 1*).³ This mechanism requires the assumption that the bond dissociation energy of the N–Br bond in NBS was significantly lower than that of Br–Br in molecular bromine. Goldfinger later challenged this mechanism proposing that NBS simply generates and maintains a low concentration of molecular bromine which was the active brominating reagent and that the bromine radical acts as the radical chain carrying species (*Scheme 1*).^{4,5} Subsequent demonstration that the N–Br bond dissociation energy is higher than Br–Br,^{4,5} along with several kinetic studies in the 1950s, led to the Goldfinger mechanism becoming widely accepted.^{6–8} However, since these early reports, in-depth mechanistic studies of this widely utilized reaction have remained notably absent from investigations using modern analytical techniques.

Our interest in this classical organic transformation stems from our process development efforts toward the manufacturing of AMG 423 dihydrochloride hydrate (**6**), a first in class cardiac myosin activator which is a clinical candidate for the treatment of systolic heart failure. Our recent report details the development of a six-step synthetic sequence to access commercial quantities of the drug substance in 55% overall yield.⁹ The first step in this sequence is the radical benzylic bromination of nitrotoluene derivative **1** with NBS and the radical initiator benzoyl peroxide to afford a mixture of monobromide **2** and dibromide **3** (*Scheme 1*). Selective

reduction of dibromide **3** using diethyl phosphite followed by alkylation with piperazine derivative **4** affords the key intermediate **5·HCl** in 81% yield.

During previous manufacturing campaigns, radical bromination of nitrotoluene **1** was conducted via portionwise addition of NBS. Nitrotoluene **1** was held for 1 h at $83 \pm 2^\circ\text{C}$ with the radical initiator benzoyl peroxide (3 mol %) and 0.1 equiv of NBS. Three sequential slurry charges of NBS in AcOH were then performed with hold times of 90 min between charges to ensure reaction progress and to minimize the risk of NBS accumulation. This procedure was adopted due to the exothermic nature of the reaction ($\Delta H_R = 136 \text{ kJ mol}^{-1}$). Our initial manufacturing runs, using several hundred kilograms of **1**, resulted in significantly lower isolated yields as compared to laboratory scale demonstrations (cf. 68% vs 81%). We also observed difficulties in phase separation during aqueous extraction due to precipitation of insoluble polymerized material.

To identify the root cause of these unexpected observations and to improve process understanding, an in-depth mechanistic study was conducted using *in situ* reaction kinetics and predictive modeling. Multinuclear CryoFree NMR spectroscopy was utilized to collect continuous kinetic data *at reaction concentration*, a significant advantage over standard NMR spectroscopy.¹⁰ To the best of our knowledge, this is the first demonstration of high temperature continuous CryoFree NMR spectroscopy for reaction monitoring. It should be

Received: May 29, 2020

Published: July 15, 2020



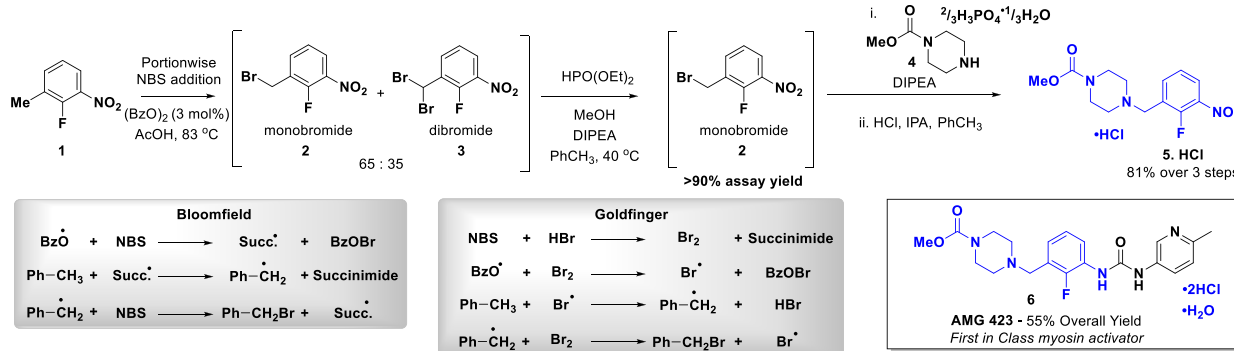
ACS Publications

© 2020 American Chemical Society

1523

<https://dx.doi.org/10.1021/acs.oprd.0c00256>
Org. Process Res. Dev. 2020, 24, 1523–1530

Scheme 1. Process To Manufacture Omecamtiv Mecarbil (6): Bloomfield and Goldfinger Proposed Mechanisms



noted that due to difficulties during the initial shimming of the spectrometer, data collected during the first ~1 h of the reaction contained large amounts of scatter and in some cases could not be collected. While in some cases this affected the overall mass balance (see *Supporting Information* for full details), kinetic data of the quality required for accurate reaction modeling were obtained.

Initial kinetic studies demonstrated that conversion of nitrotoluene 1 to monobromide 2 and dibromide 3 could be accurately monitored using ^{19}F NMR, while consumption of NBS and formation of succinimide were simultaneously determined by 1H NMR (Figure 1a). The reaction profile clearly exhibits a classic sigmoidal shape at the outset of the reaction, characteristic of the induction period expected during a chemically initiated radical process. Importantly, this simple initial experiment revealed that the rate of bromination *does not* equal the rate of succinimide formation (Figure 1b), strongly indicating the formation of an active species (i.e., Br_2) prior to bromination of the substrate.

On the basis of the successfully demonstrated use of CryoFree NMR for accurate reaction monitoring, a combination of Reaction Progress Kinetic Analysis (RPKA)^{11,12} and Variable Time Normalization Analysis (VTNA)^{13–16} were used to determine the order of each species in this reaction (Figure 2). Different Excess experiments investigate the order of each species by determining the effect of changing the concentration of each component on the global reaction rate. VTNA allows accurate mathematical derivatization of the numerical value associated with the order of each species by searching for overlay in reaction profiles via manipulation of the time axis. While, the true chemical order of a species must be an integer for an elementary reaction, VTNA allows calculation of the *observed* order which may be a noninteger and is particularly useful for kinetic modeling.

Conducting a “Different Excess” experiment by reducing the initial concentration of nitrotoluene 1 by 60% resulted in a significant decrease in reaction rate (Figure 2a). VTNA demonstrated that the reaction profiles exhibited excellent overlay in monobromide 2 formation with the observed order in nitrotoluene 1 set to $n = 1.3$. This indicates that nitrotoluene 1 is involved in the rate-determining step of this reaction.

A further “Different Excess” experiment to investigate the reaction order with respect to NBS revealed a zero-order regime during the induction period, followed by overall first-order kinetics (Figure 2b). This is indicative of formation of the active reagent bromine during induction which is then rapidly consumed during reaction progress. As bromine is consumed, HBr is produced and rapidly reacts with NBS

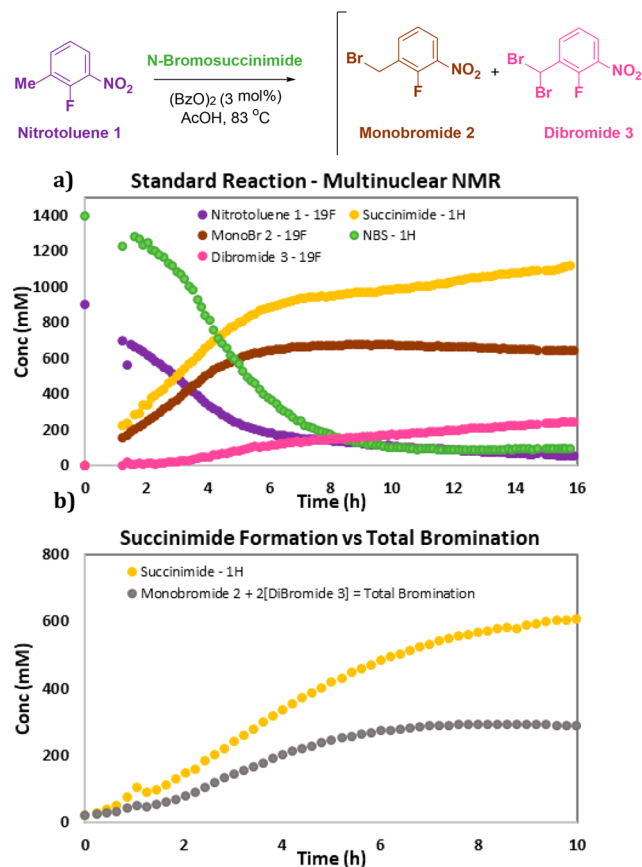


Figure 1. (a) CryoFree NMR monitoring of standard reaction conditions; $[1]_0 = 0.9$ M; $[NBS]_0 = 1.51$ M; $[(BzO)_2] = 27$ mM; d_3 -AcOD 83 °C. (b) Rate of succinimide formation vs total bromination at 0.5× reaction concentration; $[1]_0 = 0.45$ M; $[NBS]_0 = 0.76$ M; $[(BzO)_2] = 13.5$ mM; d_3 -AcOD 83 °C.

resulting in apparent first-order kinetics. VTNA exemplifies these kinetic features further by exhibiting excellent overlay for first-order kinetics during reaction progress while displaying poor overlay during the induction period.

Finally, the order in the radical initiator dibenzyl peroxide $((BzO)_2$) was investigated. Increasing the concentration of $(BzO)_2$ resulted in an increased reaction rate; however, VTNA treatment as a *catalyst of constant concentration* with an order of 0.5 (release of 2 radicals per $(BzO)_2$) exhibits poor overlay (Figure 2c). When accounting for the expected first-order radical decomposition of $(BzO)_2$ which results in a constantly decreasing concentration of $(BzO)_2$ during reaction progress,

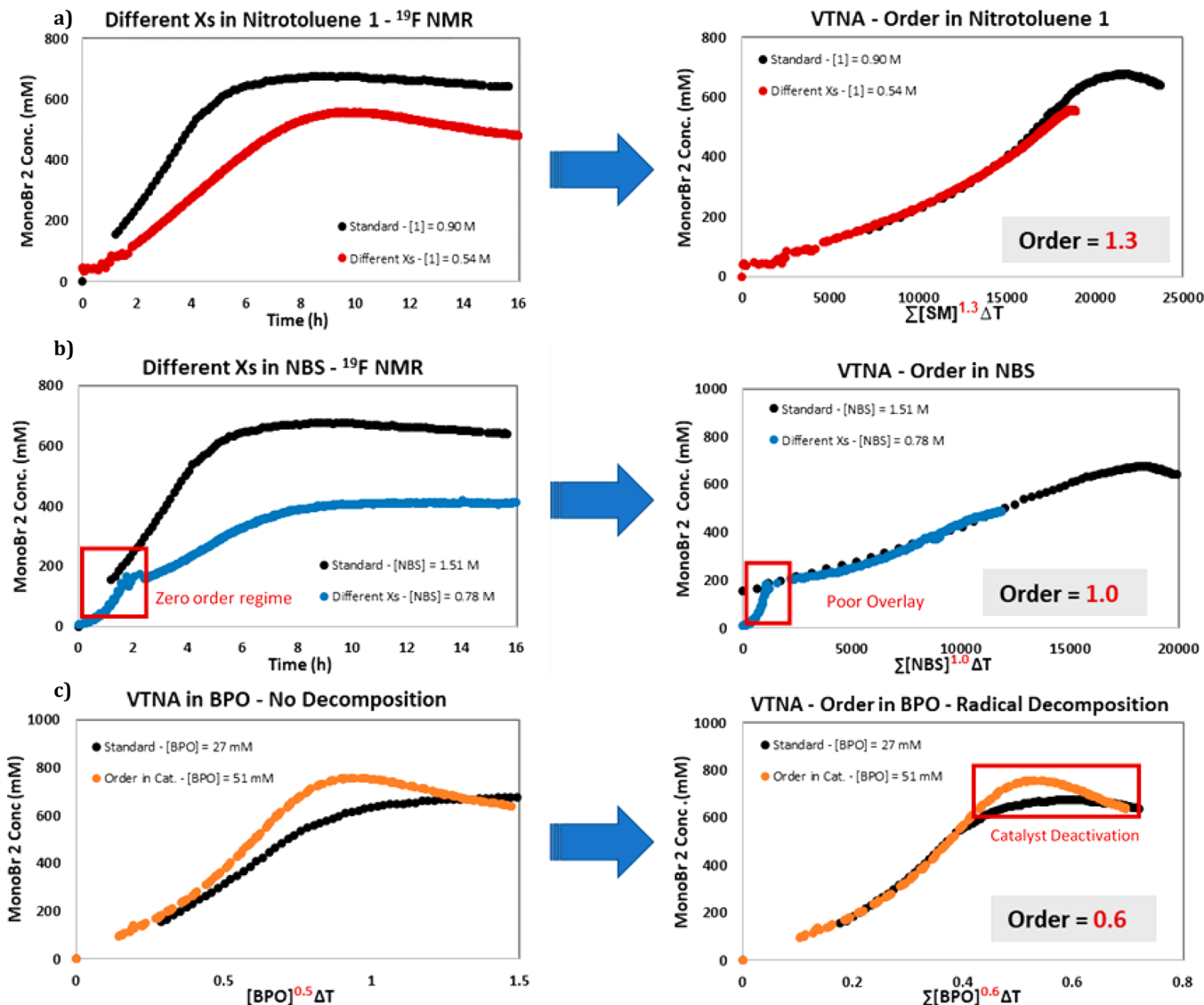
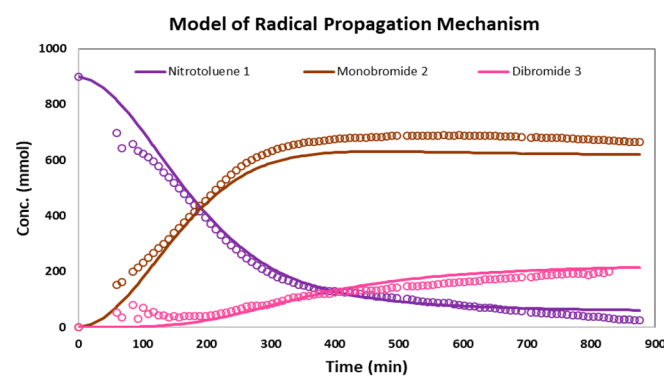


Figure 2. (a) RPKA/VTNA of different excess in nitrotoluene. (b) RPKA/VTNA of different excess in NBS. (c) VTNA of different excess in BPO accounting for decreasing [BPO] due to radical decomposition. See [Supporting Information](#) for full experimental details and complete reaction progress data ($^1\text{H}/^{19}\text{F}$ NMR).



	Elementary Steps	Predicted Rate
HBr + NBS	\rightarrow	$\text{Br}_2 + \text{Succ.}$ $4.43 \times 10^{-3} \text{ L mol}^{-1} \text{s}^{-1}$
$(\text{BzO})_2$	\rightarrow	2BzO^\bullet $1.31 \times 10^{-5} \text{ s}^{-1} (n=0.6)$
$\text{BzO}^\bullet + \text{Br}_2$	\rightarrow	$\text{Br}^\bullet + \text{BzOBr}$ $29.98 \text{ L mol}^{-1} \text{s}^{-1}$
$\text{SM 1}^\bullet + \text{Br}^\bullet$	\rightarrow	$\text{SM 1}^\bullet + \text{HBr}$ $8.89 \text{ L mol}^{-1} \text{s}^{-1} (n=1.3)$
$\text{SM 1}^\bullet + \text{Br}_2$	\rightarrow	$\text{MonoBr 2}^\bullet + \text{Br}^\bullet$ $12.86 \text{ L mol}^{-1} \text{s}^{-1}$
$\text{MonoBr 2}^\bullet + \text{Br}_2$	\rightarrow	$\text{MonoBr 2}^\bullet + \text{HBr}$ $1.47 \text{ L mol}^{-1} \text{s}^{-1}$
2Br_2	\rightarrow	$\text{Dibromide 3} + \text{Br}^\bullet$ $3.54 \text{ L mol}^{-1} \text{s}^{-1}$
Br sink	\rightarrow	Br sink $26.39 \text{ L mol}^{-1} \text{s}^{-1}$
Br sink	\rightarrow	2Br_2 $2.99 \times 10^{-5} \text{ L mol}^{-1} \text{s}^{-1}$

Figure 3. Kinetic modeling of standard reaction conditions in single batch system using data from RPKA studies.

VTNA exhibits excellent overlay for an observed order of 0.6 with respect to $(\text{BzO})_2$.¹⁶ Importantly, this analysis also

indicates that toward the end of the reaction $(\text{BzO})_2$ is no longer active as a radical initiator (Figure 2d).

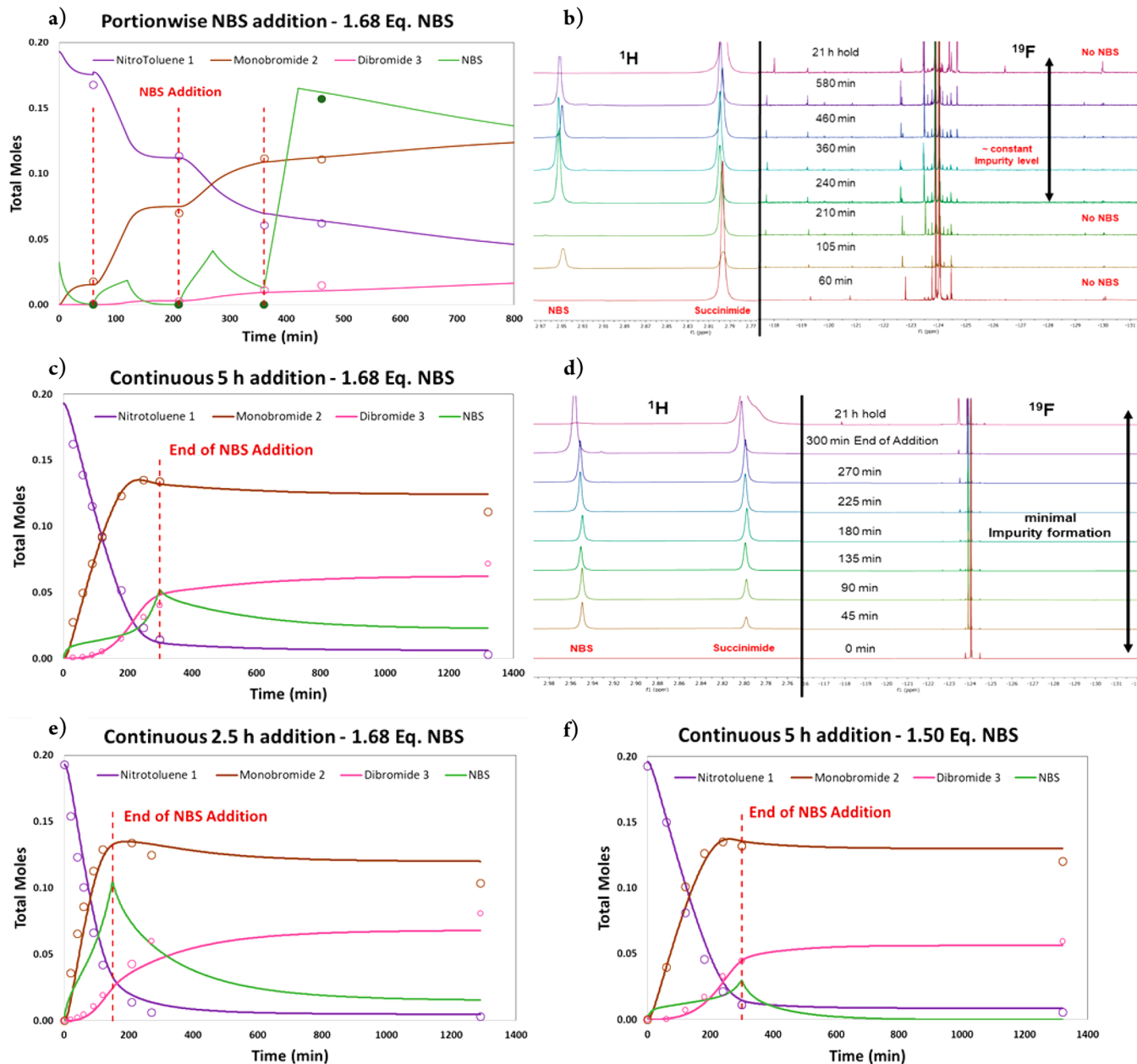


Figure 4. Prediction vs experimental data for system performance. (a) Portionwise addition of 1.68 equiv of NBS. (b) $^1\text{H}/^{19}\text{F}$ NMR aliquot analysis of reaction mixture during portionwise NBS addition. (c) 5 h Continuous addition of 1.68 equiv of NBS. (d) $^1\text{H}/^{19}\text{F}$ NMR aliquot analysis of reaction mixture during continuous 5 h NBS addition. (e) 2.5 h Continuous addition of 1.68 equiv of NBS. (f) 5 h Continuous addition of 1.50 equiv of NBS. Lines represent predicted data, and circles represent experimental data.

These initial kinetic studies revealed important considerations for effective scale-up of this process. Br_2 is the active brominating species; with a boiling point of 59 °C and a reaction temperature of 83 °C, loss of the active reagent from the solution to gas phase during reaction progress should be considered. Nitrotoluene 1 is involved in the RDS of this process and undergoes undesired arylation and polymerization in the presence of the radical initiator (benzoyl peroxide) and absence of NBS/ Br_2 . VTNA revealed that the productive reaction is first order in NBS. As such, understanding and control of both NBS and Br_2 concentration during reaction progress are essential for the successful development of a scalable and robust chemical process.

Given the plethora of kinetic data acquired during RPKA/VTNA studies, a kinetic model could be rapidly developed to

fit the experimental data using DynoChem (Figure 3).¹⁷ The Goldfinger radical propagation mechanism^{4,5} was employed using Br_2 as the active brominating agent (Scheme 1). As determined by VTNA, the reaction order was fixed with respect to nitrotoluene 1 ($n = 1.3$) and benzoyl peroxide ($n = 0.6$). To account for possible losses of the active reagent bromine to the gas phase, without introducing unnecessary complexities, this kinetic model included a ‘bromine sink.’ This introduced a second-order $[\text{Br}_2]$ dependent rate expression to account for inactivation of Br_2 . In analogy to loss of Br_2 gas to the reactor headspace, this model allowed for slow reintroduction of Br_2 to the system (see Supporting Information for details).

The reaction rate predictions from kinetic modeling suggested that NBS/ Br_2 would be consumed between NBS

Table 1. Composition of Final Reaction Mixture after Continuous Addition of NBS Compared with Portionwise Addition^a

Entry	NBS Addition Time	Time (h)	¹⁹ F NMR (%)			
			NitroTol 1	MonoBr 2	DiBr 3	Impurities
1	5.5 h	5	7.55	69.41	21.08	1.96
		21	1.76	57.50	37.20	3.54
2	Portionwise (Standard) ^b	5	14.37	67.95	13.55	4.13
		21	1.79	56.36	33.43	8.42
3	Portionwise (Extended) ^b	5	27.53	60.29	7.00	5.18
		21	0.82	52.54	36.52	10.12

^aImage 1: Polymerized material precipitating during aqueous extraction from portionwise extended reaction (Table 1, entry 3); see Supporting Information for further information. ^bHold period between charges of NBS increased from 90 min (standard) to 180 min for “extended” portionwise addition.

charges during the portionwise charges adopted during our initial manufacturing campaign. With the understanding that nitrotoluene **1** is involved in the RDS of this process, it seemed likely that impurity generation/polymerization would be exacerbated during the absence of the active reagent Br₂. To investigate this further, we applied our kinetic model to the portionwise NBS addition mode for comparison of the predicted and experimental data (Figure 4a and b).

Pleasingly, the kinetic model for portionwise addition accurately described the observations during aliquot analysis, successfully predicting that NBS consumption would occur prior to the first and second slurry charges and that conversion of nitrotoluene **1** to monobromide **2** would cease during this time (Figure 4a and b). ¹⁹F NMR aliquot analysis demonstrated that that impurity generation was most prevalent during this stalling of reaction progress, and ¹H NMR identified extended periods of time during which NBS was absent from the reaction mixture. Importantly, significant impurity formation occurred during the initial heating of nitrotoluene **1** in the presence of benzyl peroxide for 60 min prior to the first NBS charge. Formation of polymerized impurities were also verified to result from prolonged exposure of nitrotoluene **1** to (BzO)₂ and exacerbated in the absence of NBS.

To account for these considerations and improve process performance, we proposed the adoption of a slow, continuous addition of the NBS slurry. This would maintain a consistent source of NBS, minimizing polymerization and impurity formation. A low concentration of NBS would also ensure a low concentration of the active reagent Br₂ which would be rapidly consumed by nitrotoluene **1** minimizing the loss of this reagent from the solution phase. Understanding the reaction rates with regards to NBS consumption also allowed introduction of a controlled NBS addition rate, ensuring the desired productive reaction would be driven forward by maintaining a low NBS/Br₂ concentration while preventing hazardous accumulation of NBS in the reactor. From a

commercial production and engineering perspective, 5 h was targeted as an achievable addition time given the volume of ambient temperature NBS/AcOH slurry to be charged while maintaining a reaction temperature of 83 °C.

The prediction of system performance using a continuous addition model was in excellent agreement with experimental data. In contrast to portionwise addition, aliquot analysis using ¹H NMR demonstrated the consistent presence of NBS in the solution phase. Concurrently, ¹⁹F NMR analysis demonstrated a vast improvement in the absolute purity of the reaction mixture, with minimal impurity formation occurring during the process.

The continuous addition model allowed accurate prediction and experimental confirmation that the end of reaction specifications (<3 LC area percent; <8 mol % nitrotoluene **1**) would be consistently achieved <1 h after NBS addition was complete across the range of addition times (2.5–8 h) and NBS equivalents (1.5–1.9). Importantly, this demonstrated that under the continuous addition mode reaction progress was controlled by NBS addition rate. Maximal conversion of nitrotoluene **1** was achieved toward the end of NBS addition, providing a significant reduction in reaction time (cf. 21 h using portionwise addition). As such, continuous addition of NBS could now be successfully conducted within the wide operating parameters desired for a manufacturing setting.

In line with our original hypothesis, slow addition of NBS resulted in a significant reduction in impurity formation (Figure 4d, cf. Figure 4b). While at the end of reaction monitoring (time = 21 h) similar levels of monobromide **2** and dibromide **3** were observed across addition modes, NMR analysis of the final reaction mixture composition revealed that continuous addition of NBS reduced impurity formation by ~50% (entry 1 vs 2, Table 1). This can be reduced further considering the end of reaction specifications are met <1 h after continuous addition of NBS is complete. We also demonstrated that increasing the time between NBS charges increased impurity formation to >10% (¹⁹F NMR) and

resulted in precipitation of polymeric species during aqueous extraction (entry 3, Table 1 and Image 1). These observations were in line with those made during the previous manufacturing campaign.

Having experimentally demonstrated the accuracy of our kinetic model across addition modes, we utilized its predictive power to model the concentration of the active reagent Br_2 during reaction progress (Figure 5). Portionwise addition of

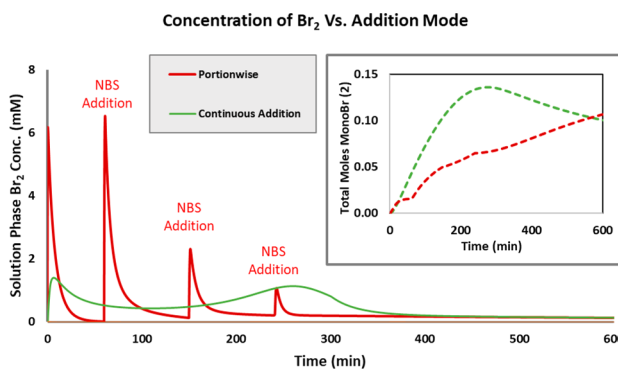


Figure 5. Kinetic Modeling of Br_2 concentration during portionwise (red) and 5 h continuous (green) addition of NBS.

NBS results in rapid generation of Br_2 with each NBS charge. During these peaks in $[\text{Br}_2]$ our kinetic model predicts that Br_2 is lost from the solution to gas phase ("bromine sink"); as such, no increase in monobromide **2** formation is observed during these peaks. In contrast, during continuous addition a low $[\text{Br}_2]$ is consistently maintained in the presence of high [nitrotoluene **1**] resulting in rapid consumption of Br_2 as NBS is introduced to the system. As a result, monobromide **2** formation occurs more efficiently during continuous addition of NBS.

The accumulation of Br_2 predicted to occur in the gas phase during portionwise addition implies that reactor fill volume is an important consideration for this process. This parameter likely played a role in the variations observed during our initial manufacturing campaigns in which the vessel fill volume was less than 30%, leading to the formation of polymerized material and low isolated yield of **5·HCl**. The influence of this parameter should be minimized using continuous NBS addition by ensuring rapid consumption of Br_2 . To investigate this, the effect of fill volume on the final reaction mixture composition was compared across portionwise and continuous addition modes (Table 2).

Using portionwise addition mode, increasing the fill volume from 17% to 48% resulted in a 50% reduction in impurity formation (entry 1 vs 2, Table 2). Incorporation of a strong nitrogen flow through the headspace of the reactor during reaction progress significantly inhibited the productive reaction and resulted in >20% impurity formation, presumably as a result of Br_2 removal from the system. These results demonstrate that accumulation of Br_2 occurs during portionwise addition of NBS and that this reagent can escape the solution phase under the reaction conditions. In contrast, using continuous NBS addition, fill volume and N_2 sweeping had negligible effect on the final reaction mixture composition, demonstrating that rapid consumption of Br_2 occurs in the solution phase and minimizing escape of this reagent to the gas phase.

Table 2. Comparison of Fill Volume Effect Using Portionwise and Continuous NBS Addition

entry	addition mode	fill volume (%)	final reaction composition (%) ^a		
			SM 1	P (2 + 3)	impurities
1	portionwise	17	6.8	85.6	7.6
2		48	5.0	91.3	3.7
3		48 ($\uparrow \text{N}_2$ flow) ^b	27.6	50.6	21.8
4	continuous	25	2.0	95.2	2.8
5		48	3.8	94.1	2.1
6		48 ($\uparrow \text{N}_2$ flow) ^b	5.5	92.2	2.3

^aDetermined by ^{19}F NMR spectroscopy of crude reaction mixture after 21 h. ^bStrong nitrogen sweep applied through headspace of reactor.

Having determined the root cause of the low isolated yield and polymerized byproducts in our previous manufacturing campaign were a result of starving the reaction mixture of the active reagent Br_2 , we were prompted to understand better a separate concern. We observed differing levels of bromination using NBS from different suppliers. While nitrotoluene **1** consumption was in line with in-house observations, final ratios of monobromide **2** and dibromide **3** demonstrated consistently higher levels of overall bromination. The source of this increased activity was the result of variable quality of NBS from different suppliers with regards to Br_2/HBr content (Table 3).¹⁸ Indeed, NBS from Supplier B resulted in an increase of >8 LC area % of dibromide in comparison to our original studies using NBS from Supplier A.

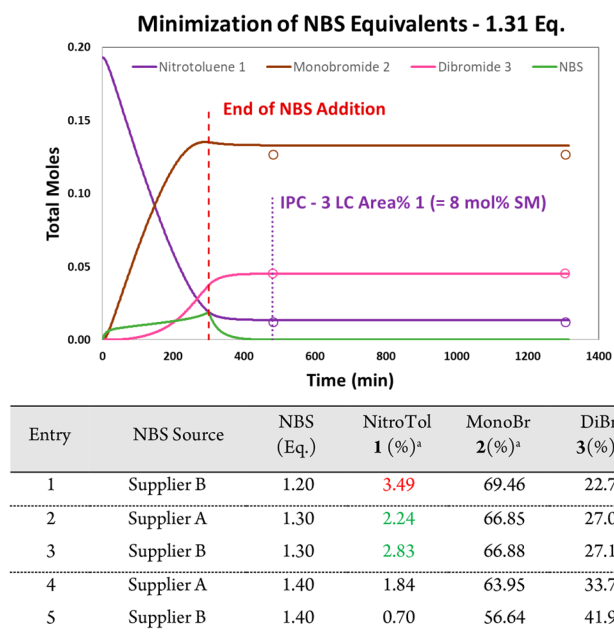
Table 3. Effect of Variation in Br_2 Content on NBS Activity

entry	NBS source ^a	NitroTol 1 (%) ^b	MonoBr 2 (%) ^b	DiBr 3 (%) ^b	Br in NBS (%) ^c
1	Supplier A	0.97	59.13	38.24	0.234
2	Supplier B	0.81	52.01	46.39	0.748

^aUsing 1.5 equiv of NBS added over 5 h. ^bLC area %. ^cMol % determined by UV-vis spectrometry.

NBS with elevated levels of Br_2/HBr was found to be more active in this radical bromination due to the inherent rate-determining effect of these species in the reaction mechanism. These species act to reduce the observed induction period, increase the overall reaction rate, and result in increased levels of dibromide **3**. In our manufacturing process, the final mono-to dibromide ratio must be carefully controlled as the subsequent transformation in our telescoped three-step process to access nitropiperazine **5·HCl** (Scheme 1) involves reduction of dibromide **3** to monobromide **2** with diethylphosphite (0.44 equiv). Aware that NBS quality for commercial manufacturing may be variable, we opted to minimize NBS equivalents while ensuring reaction completion accounting for variable NBS quality. To do so, we utilized our kinetic model for optimization, minimizing NBS equivalents while ensuring the reaction would pass the "in-process control" IPC, <3 LC area percent nitrotoluene **1** 3 h after NBS addition was complete. Modeled optimization predicted 1.31 equiv of NBS would be required to pass the IPC after 8 h with a 5 h continuous addition mode (Table 4; see Supporting Information for full details of modeling optimization). This is in excellent agreement with experimental data which demonstrated successful reaction completion using 1.30 equiv of NBS from

Table 4. Predicted vs Experimental Minimization of NBS Equivalents



^aLC area %; <3 LC area % = <8 mol % starting material required to pass IPC.

both sources and that the reaction failed to meet the completion specifications using 1.20 equiv of the “more active” NBS from Supplier B. As such, NBS equivalents were conservatively reduced from 1.68 to 1.40 equiv for the final manufacturing process.

In conclusion, the initial manufacturing campaign for a radical benzylic bromination resulted in several unexpected observations that warranted an in-depth mechanistic analysis of the process. Multinuclear CryoFree NMR spectroscopy was employed to conduct kinetic analysis and develop an accurate and predictive mechanistic model. This revealed that Br₂ is the active brominating agent and that our previously employed portionwise addition protocol resulted in the absence of the active brominating agent from the reaction mixture for prolonged periods of time during the process. This absence of reagent led to the formation of polymerized material and associated low yield of the desired product. Increased kinetic and mechanistic understanding led to the adoption of a continuous slurry addition of NBS which was demonstrated to minimize impurity formation and polymerization by maintaining a low solution phase concentration of Br₂. This resulted in rapid consumption of the active reagent Br₂ and minimizing losses of this reagent from the solution phase. Continuous addition of NBS also allowed for a reduction in reaction time from 21 to 8 h, a decrease in the required equivalents of NBS from 1.68 to 1.40, and a reduction in impurity formation by >50%.

During our most recent manufacturing campaign, continuous addition of 1.40 equiv of NBS was utilized for the bromination of nitrotoluene **1**. Pleasingly, minimal variation in final reaction mixture composition was observed, demonstrating consistent consumption of nitrotoluene **1** and mono- to dibromide ratio across multiple batches on >200 kg scale. Precipitation of polymerized material during aqueous extraction was not problematic and allowed for facile phase

separation. Polymerized material was not detected in the final isolated solid (cf. 2 wt % in previous campaign). While in the previous manufacturing campaign portionwise NBS addition resulted in the final isolated yields <70%, simple adoption of a continuous NBS addition reproducibly increased this yield to 75–80%.

■ ASSOCIATED CONTENT

SI Supporting Information

The Supporting Information is available free of charge at <https://pubs.acs.org/doi/10.1021/acs.oprd.0c00256>.

Full details of CryoFree NMR spectroscopy, portionwise and continuous addition protocols; all data associated to these experiments and the kinetic model including predictions ([PDF](#))

■ AUTHOR INFORMATION

Corresponding Author

James I. Murray — *Pivotal and Commercial Drug Substance Technologies, Process Development, Amgen Inc., Thousand Oaks, California 91320, United States;* orcid.org/0000-0002-8668-9261; Email: j.murray@amgen.com

Authors

Maria V. Silva Elipe — *Attribute Sciences, Amgen Inc., Thousand Oaks, California 91320, United States;* orcid.org/0000-0002-8429-9534

Andrew Cosbie — *Pivotal and Commercial Drug Substance Technologies, Process Development, Amgen Inc., Thousand Oaks, California 91320, United States*

Kyle Baucom — *Pivotal and Commercial Drug Substance Technologies, Process Development, Amgen Inc., Thousand Oaks, California 91320, United States*

Kyle Quasdorf — *Pivotal and Commercial Drug Substance Technologies, Process Development, Amgen Inc., Thousand Oaks, California 91320, United States*

Seb Caille — *Pivotal and Commercial Drug Substance Technologies, Process Development, Amgen Inc., Thousand Oaks, California 91320, United States;* orcid.org/0001-5434-5483

Complete contact information is available at:
<https://pubs.acs.org/10.1021/acs.oprd.0c00256>

Notes

The authors declare no competing financial interest.

■ REFERENCES

- (1) Wohl, A. Bromierung Ungesättigter Verbindungen Mit N-Bromacetamid, Ein Beitrag Zur Lehre Vom Verlauf Chemischer Vorgänge. *Ber. Dtsch. Chem. Ges. B* **1919**, *52*, 51–63.
- (2) A Scifinder structure search for benzylic bromination using NBS and a chemical initiator reveals more than 12,000 examples as of January 2020.
- (3) Bloomfield, G. F. 43. Rubber, Polyisoprenes, and Allied Compounds. Part VI. The Mechanism of Halogen-Substitution Reactions, and the Additive Halogenation of Rubber and of Dihydromyrcene. *J. Chem. Soc.* **1944**, 114.
- (4) Adam, J.; Gosselain, P. A.; Goldfinger, P. Laws of Addition and Substitution in Atomic Reactions of Halogens. *Nature* **1953**, *171*, 704–705.
- (5) Goldfinger, P.; Gosselain, P. A.; Martin, R. H. Induction Periods in Reactions of N-Halogenimides. *Nature* **1951**, *168*, 30–32.

- (6) Dauben, H. J.; McCoy, L. L. N-Bromosuccinimide. II. Allylic Bromination of Tertiary Hydrogens. *J. Org. Chem.* **1959**, *24*, 1577–1579.
- (7) Pearson, R. E.; Martin, J. C. The Mechanism of Benzylic Bromination with N-Bromosuccinimide. *J. Am. Chem. Soc.* **1963**, *85*, 354–355.
- (8) Russell, G. A.; DeBoer, C.; Desmond, K. M. Mechanisms of Benzylic Bromination. *J. Am. Chem. Soc.* **1963**, *85*, 365–366.
- (9) Caille, S.; Algeier, A. M.; Bernard, C.; Correll, T. L.; Cosbie, A.; Crockett, R. D.; Cui, S.; Faul, M. M.; Hansen, K. B.; Huggins, S. Development of a Factory Process for Omecamtiv Mecarbil, a Novel Cardiac Myosin Activator. *Org. Process Res. Dev.* **2019**, *23*, 1558–1567.
- (10) Silva Elipe, M. V.; Donovan, N.; Krull, R.; Pooke, D.; Colson, K. L. Performance of new 400-MHz HTS power-driven magnet NMR technology on typical pharmaceutical API, cinacalcet HCl. *Magn. Reson. Chem.* **2018**, *56*, 817–825.
- (11) Blackmond, D. G. Reaction Progress Kinetic Analysis: A Powerful Methodology for Mechanistic Studies of Complex Catalytic Reactions. *Angew. Chem., Int. Ed.* **2005**, *44*, 4302–4320.
- (12) Blackmond, D. G. Kinetic Profiling of Catalytic Organic Reactions as a Mechanistic Tool. *J. Am. Chem. Soc.* **2015**, *137*, 10852–10866.
- (13) Burés, J. A Simple Graphical Method to Determine the Order of a Reaction in Catalyst. *Angew. Chem., Int. Ed.* **2016**, *55*, 2028–2031.
- (14) Burés, J. What Is the Order of a Reaction? *Top. Catal.* **2017**, *60*, 631–633.
- (15) Nielsen, C. D.-T.; Burés, J. Visual Kinetic Analysis. *Chem. Sci.* **2019**, *10*, 348–353.
- (16) Martínez-Carrión, A.; Howlett, M. G.; Alamillo-Ferrer, C.; Clayton, A. D.; Bourne, R. A.; Codina, A.; Vidal-Ferran, A.; Adams, R. W.; Burés, J. Kinetic Treatments for Catalyst Activation and Deactivation Processes based on Variable Time Normalization Analysis. *Angew. Chem., Int. Ed.* **2019**, *58*, 10189.
- (17) DynoChem, Scale-Up Systems Ltd., Build: 1.3.20b340, Data Version: 1.0. 2020.
- (18) Bonfield, H. E.; Williams, J. D.; Ooi, W. X.; Leach, S. G.; Kerr, W. J.; Edwards, L. J. A Detailed Study of Irradiation Requirements Towards an Efficient Photochemical Wohl-Ziegler Procedure in Flow. *ChemPhotoChem.* **2018**, *2*, 938–944.